Materials Science-Poland, *Vol. 26*, *No. 1*, *2008*

Application of microelectrodes for investigation of the oxygen electrode reaction in selected solid electrolytes

A. RAŹNIAK*, P. TOMCZYK

Faculty of Fuels and Energy, AGH University of Science and Technology,
al. Mickiewicza 30, 30-059 Krakow, Poland,

In a solid oxide fuel cell (SOFC), the most often used solid electrolyte is yttria stabilized zirconia. Usually, SOFC of a tubular geometry operates at ca. 1000 °C. To decrease the temperature of the cell, it is necessary to reduce the thickness of electrolyte or replace yttrium-stabilized zirconium with an other electrolyte of a much higher ionic conductivity. A potential candidate for an electrolyte in intermediate temperature SOFC is gadolinia doped ceria. The largest energetic losses in a fuel cell of this type, apart of ohmic polarizations, are attributed to slow kinetics of the cathodic process. In this work, investigated oxygen electrode reaction for two various electrolytes: yttria stabilized zirconia and gadolinia doped ceria. The measurements were conducted using microelectrodes for which analysis of kinetic parameters of the electrode reaction is easier. Gold electrodes were applied in the experiments. Although Au is a good electrocatalyst for oxygen reduction, almost no research has been done for this metal so far. The performance of the electrode and results of impedance measurements have been presented and discussed.

Key words: *fuel cell; oxygen electrode; microelectrode; solid electrolyte; YSZ; GDC*

1. Introduction

Solid electrolytes with high oxygen ion conductivity are of special interest for their application in high temperature electrochemical systems such as solid oxide fuel cells (SOFC), oxygen sensors and oxygen pumps. Fuel cells are efficient generators of electric energy. They are usually fed with a fuel produced by reforming of natural gas. Among fuel cells, SOFCs are one of the most promising energy converters with a great potential for high efficiency and low pollution [1, 2]. Generally, yttria stabilized zirconia (YSZ) is used as an electrolyte material in SOFCs operating at 800–1000 °C. Reduction of the operating temperature allows one to use cheaper construction materials and more reliable seals in the cell. Thus, investigations aimed at de-

*Corresponding author, e-mail: razniak@agh.edu.pl

creasing the operating temperature down to 500–700 °C are often focused on new electrolyte materials [3]. Gadolinia (CGO) or samaria doped ceria (CSO) are attractive candidates for electrolytes which could be employed in the intermediate temperature solid oxide fuel cells (IT-SOFC). IT-SOFC can be used in small scale combined heat and power applications (e.g., stand-alone residential units), remote location power generators and also for transport means [4, 5].

Although the thermodynamics of YSZ and gadolinia doped ceria (GDC) is well understood, a controversy still persists on the mechanism and kinetics of the electrode processes occurring in these electrolytes. The most extensive research into processes occurring in SOFC has been made, by an analogy to a state-of-the-art fuel cell, for porous electrodes. One of possible reasons for unsatisfactory understanding of the oxygen electrode reaction in solid ionics is the fact that porous electrodes have complex and difficult to determine structure and geometry. To avoid problems associated with porous electrodes at solid state electrolytes, a number of researchers have used a concept of microelectrodes, well known from liquid electrochemistry. In the solid state electrochemistry, the microelectrodes are frequently applied in polymer electrolytes whereas they are less commonly employed in ionic solids.

2. Experimental

This work is aimed at comparison of the kinetic parameters of the oxygen electrode reaction occurring in two solid electrolytes (YSZ and GDC) in analogous conditions. The work was done, first of all, for Au quasi-point electrodes because of two reasons:

- Regarding metallic electrodes, the papers published to date described almost exclusively the behaviour of Pt microelectrodes [6–8]. It is of interest to examine phenomena occurring at the microelectrodes made of materials other than Pt, e.g. Au, which is not much worse electrocatalyst for the oxygen electrode reaction than Pt.
- Au is more plastic than Pt at high temperatures. Therefore, in the conditions of high temperature measurement, a well defined contact between this metal and the electrolyte can be formed easier than in the case of Pt needle.

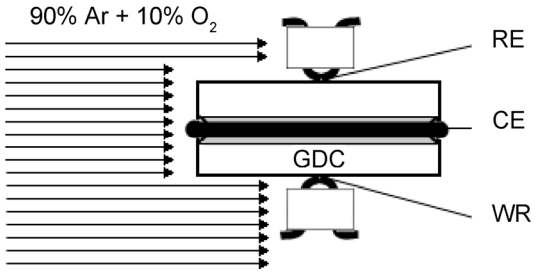

Fig. 1. Side view of the measurement cell: RE – reference electrode, CE – counter electrode, WR – working electrode

The side view of the measurement cell is shown in Fig. 1. The YSZ and GDC disks (10 mm in diameter and ca. 3 mm thick) were formed from powdered com-

pounds pressed isostatically under 250 MPa. Then, the samples were sintered for 2 h at 1500 °C in air. A co-precipitation calcination method was used to prepare powders of gadolinia doped ceria (with 20% mol Gd_2O_3) and yttria stabilized zirconia (8% mol Y_2O_3). Both disks were produced at the Faculty of Materials Science and Ceramics of AGH, University of Science and Technology in Cracow. The procedure was similar to this described in papers [9–11]. The XRD method was used to determine cell parameters of the samples.

Both flat sides of the disk were polished with a 2000 waterproof alumina abrasive paper and afterwards with 1 μm diamond paste. Two quasi-point electrodes were placed at the polished surfaces, one opposite to the other as is shown in Fig. 1. The quasi-point electrode was made by passing a wire 0.3 mm in diameter throughout two holes of alumina bead – one electrode was made of gold wire (working electrode) and the other from platinum wire (reference electrode). The platinum wire (0.3 mm in diameter), which was used as a counter electrode, was placed in a furrow grooved around the side surface of the disk just in the middle of the side. To improve contact between the Pt wire and the electrolyte, the furrow was smeared with a platinum paste. The electrodes and disk were assembled inside an alumina holder and gripped together due to action of springs with a force of about 0.5 N. The cell with the holder was then placed inside an alumina envelope, which provided a gas-tight separation from the outer atmosphere. Finally, the whole system was put into a horizontal electric furnace. An inlet of the gases was located a few millimeters from the side wall of the disk providing the gases to flow directly to the electrodes. A set up of gas flow controllers allowed one to control the composition and flow rates of gases introduced into the cell.

Before the experiment, the cell was heated to 900–1000°C and held at this temperature for about one hour. In these conditions, gold and platinum became soft and the quasi-point electrodes, pressed by the springs to the disk, increased contact areas between the metal and electrolyte. The contact areas and lengths of three phase boundaries could be determined after completing the experiments, when the cell was disassembled and the electrodes were examined with a scanning microscope.

The flattened part of the metal surface corresponded to the area being in direct contact with the electrolyte. An example of the view of the Au electrode after completing experiment with GDC electrolyte is shown in Fig. 2. In this case, the contact area of the Au electrode and length of three phase boundary were estimated geometrically at 0.15 mm^2 and 1.62 mm, respectively. All electrochemical experiments were performed at 700 °C under atmosphere of $0.1O_2$ + 0.9Ar at ambient pressure. The flow rate of the gases into the electrochemical cell was equal to 50 cm^3/min. The potential of the Au working electrode was measured vs. the reference platinum quasi-point electrode, located at the opposite side of the disk. The chronoamperometric (CA) and electrochemical impedance spectroscopy (EIS) techniques were used in the measurements. Due to long-term effects of the electrode polarization, the dependences of the current on the time of polarization were recorded during at least 15 h. In the CA experiments, the microelectrodes were polarized stepwise from the rest potential down to –0.3 V

(for GDC to –0.6 V). To get additional information, the EIS was applied to determine and characterize the impedance of the electrode before the polarization and at the end of the potential step.

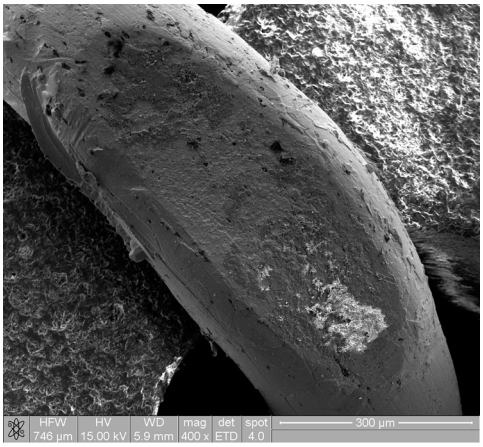

Fig. 2. SEM images of the flattened part of the Au electrode

The samples were measured with GPES (CA) and FRA (EIS) modules of an Autolab PGSTAT 30 interfaced with a computer. The impedance spectroscopy measurements were performed in the frequency range from 0.001 Hz to 1 MHz using 10 mV amplitude of the sinusoidal voltage. For analysis of the impedance data, a program provided by the producer based on a complex non-linear regression least-squares fit was used.

3. Results and discussion

According to Steele [12], the highest ionic conductivity of doped ceria is exhibited by $Ce_{0.8}Gd_{0.2}O_{2-x}$. The conductivities of gadolinia doped ceria at 700 °C determined by various authors [4, 12–20] are given in Table 1.

Table 1. Conductivities at 700 °C of gadolinia doped ceria $Ce_{0.8}Gd_{0.2}O_{2-x}$

σ_{el}/(mS·cm^{-1})	45.70	67.99	35.00	45.20	77.00	18.20	42.50	26.70	19.00	18.50	47.00	35.20
Reference	[13]	[14]	[14]	[15]	[12]	[16]	[17]	[17]	[18]	[19]	[4]	[20]

Considering the scatter in the data of conductivities (Table 1) determined by various authors, it should be emphasized that the actual values obtained are distinctly dependent on the bulk and grain boundary resistivity, i.e., they reflect different conditions of the sample fabrication [5].

In the case of metallic electrodes, the reaction occurs exclusively at the three phase boundary (TPB). Therefore, it is very important to determine the length of this boundary. The data presented further in this paper will be normalized vs. the length of TPB.

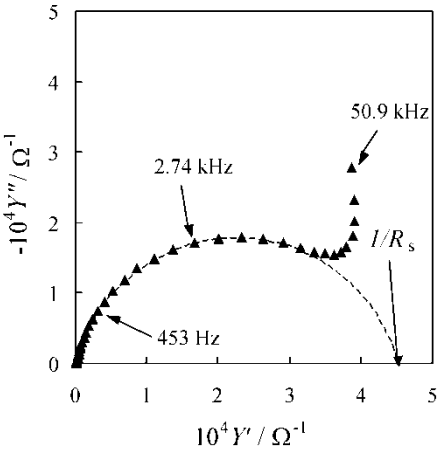

Fig. 3. Admittance complex plots for the Au quasi-point electrode placed at the YSZ electrolyte (temperature 700 °C, polarization potential –0.3 V, $p(O_2)$ = 0.1 bar)

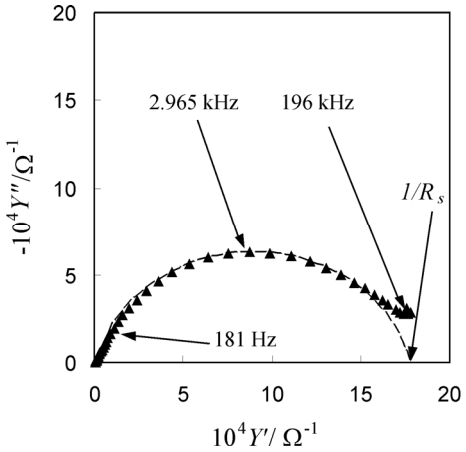

Fig. 4. Admittance complex plots for the Au quasi-point electrode placed at the GDC electrolyte (temperature 700 °C, polarization potential –0.3 V, $p(O_2)$ 0.1 bar)

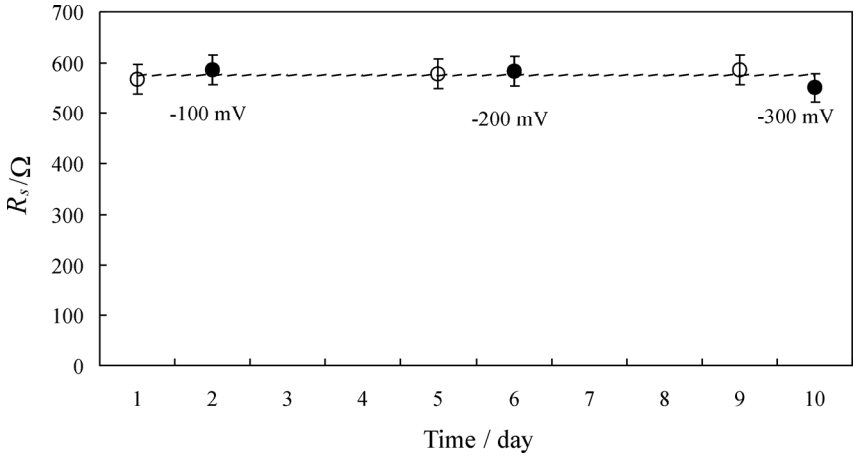

Fig. 5. R_s, resistance of the electrolyte, determined from the admittance complex plots for the Au quasi-point electrode placed at the GDC electrolyte. The empty and full circles correspond to the unpolarized and polarized electrode, respectively (temperature 700 °C, $p(O_2)$ 0.1 bar)

In Figures 3 and 4, the characteristic complex admittance plots of the Au electrode placed at the YSZ and GDC electrolytes are presented. For these plots, it is relatively easy to fit a semicircle representing polarization admittance of the oxygen electrode. The right crossing points of the semicircle with the Y' axis can by attributed to the total admittance of the electrolyte which comprises bulk and grain boundary effects. As can be seen in Fig. 5, the resistance of the electrolyte R_s, calculated from the admittance data, is independent of the duration of the experiment and polarization of the electrode. Determination of the electrode resistance from the complex impedance plots

(Figs. 6 and 7) is less precise because of a small number and uncertainty of experimental points in the required range of high frequencies.

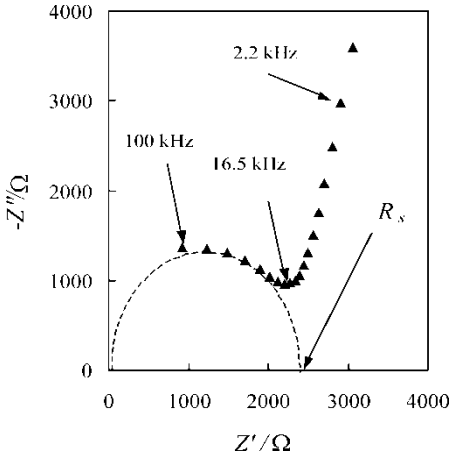

Fig. 6. Impedance complex plots for the Au quasi-point electrode placed at the YSZ electrolyte (temperature 700 °C, polarization potential –0.3 V, $p(O_2)$ = 0.1 bar)

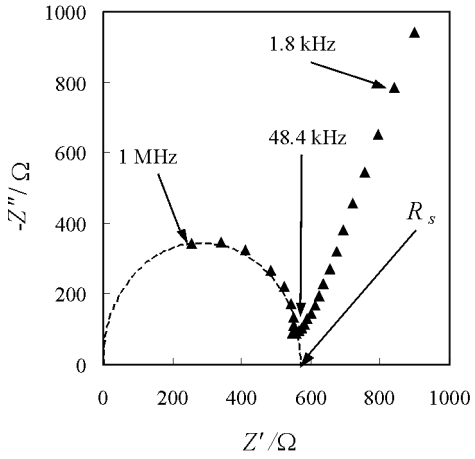

Fig. 7. Impedance complex plots for the Au quasi-point electrode placed at the GDC electrolyte (temperature 700 °C, polarization potential –0.3 V, $p(O_2)$ 0.1 bar)

For a perfectly circular point electrode, the electrolyte resistance R_s determined by the impedance spectroscopy, according to the Newman formula is equal to [21]:

$$R_s = \frac{\pi}{2 l_{\text{circle}} \sigma_{\text{el}}} \tag{1}$$

where l_{circle} is the TPB length of perfectly circular electrode and σ_{el} is the specific conductivity of the electrolyte. However, the metallic electrodes used in our work were not perfectly circular. Therefore, we have used the corrective factor

$$\gamma = \frac{l_{\text{ellipse}}}{l_{\text{circle}}} \tag{2}$$

which increases the TPB length according to the elliptical deformation of the electrode used in our experiments (Fig. 2). l_{ellipse} and l_{circle} are the perimeters of an ellipse and a circle, respectively. Hence, Eq. (1) could be rewritten for the elliptical electrodes in the form:

$$R_s = \frac{\pi}{2 \gamma l_{\text{circle}} \sigma_{\text{el}}} \tag{3}$$

The perimeter of an ellipse is approximately equal to:

$$l_{\text{ellipse}} = \pi \left[1.5 (a + b) - \sqrt{ab} \right] \tag{4}$$

where a and b are the semimajor and semiminor axes. The measure of an electrode deformation vs. the perfect circle is a factor ξ equal to the ratio of semimajor and semiminor axes:

$$\xi = \frac{a}{b} \tag{5}$$

Hence

$$\gamma = \frac{l_{\text{ellipse}}}{l_{\text{circle}}} = 0.75(\xi + 1) - 0.5\sqrt{\xi} \tag{6}$$

For all electrodes used in our experiments, the deformation factor was equal approximately to $\xi = 2.9$, hence the corrective factor was assumed to be $\gamma = 2.1$.

Taking the average value of GDC conductivities equal to $\sigma_{(\text{el})\text{av}} = 40 \pm 19$ mS·cm^{-1} from Table 1 and R_s from Fig. 5, we can estimate l_{ellipse} of our electrodes. For the example shown in Fig. 2, it was calculated to be 1.44 mm, as compared to 1.62 mm measured geometrically from the image of the flattened part of the electrode (Fig. 2). $\sigma_{\text{el}} = 32.4$ mS·cm^{-1} of our electrolyte sample was also determined directly from the EIS measurements. In this experiment, large reversible Pt electrodes were deposited on the both sides of a disk. Taking this value of the conductivity, we calculated $l_{\text{ellipse}} = 1.77$ mm. Regarding a possible scatter of the σ_{el} due to various ways of preparation, the agreement between calculated and geometrical determined values of tree phase boundary can be considered acceptable. To avoid the problems with the procedure of geometrical determination of l_{TPB} for each single electrode, we used calculated values with σ_{el} determined individually for our electrolyte sample.

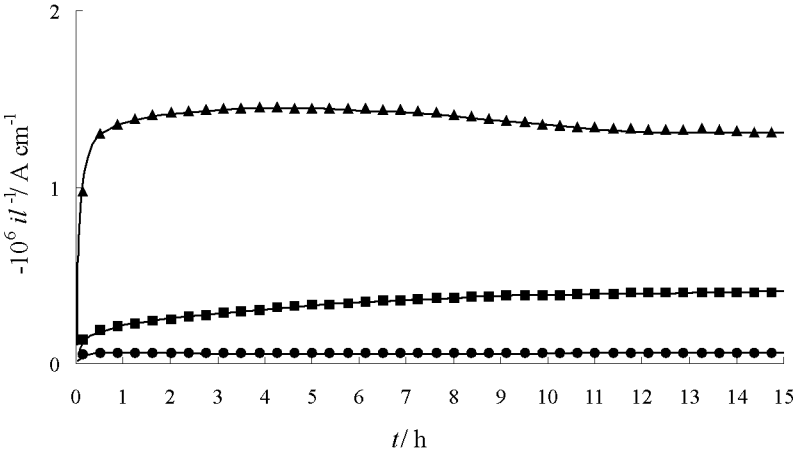

Fig. 8. Dependences of the current normalized vs. tree phase boundary length, on the time of polarization for the Au quasi-point electrode placed at the YSZ electrolyte. Triangles, squares and circles correspond to the polarization electrode potentials: –0.3 V, –0.2 V and –0.1 V, respectively, (temperature 700 °C, $p(O_2) = 0.1$ bar)

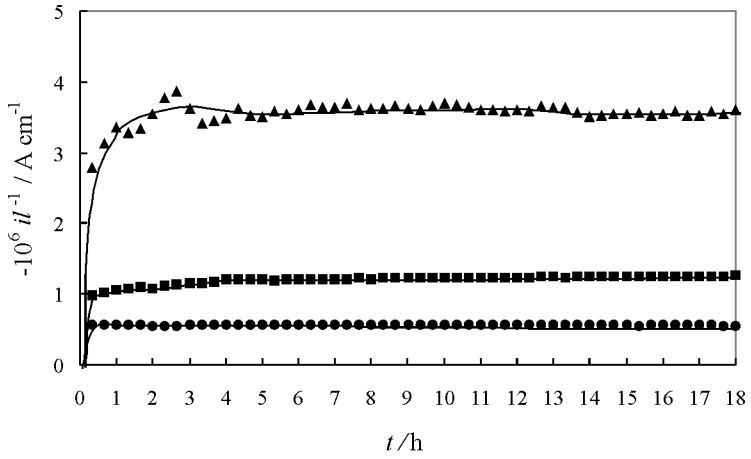

Fig. 9. Dependences of the currents normalized vs. tree phase boundary length on the time of polarization for the Au quasi-point electrode placed at the GDC electrolyte. Triangles, squares and circles correspond to the polarization electrode potentials: –0.3 V, –0.2 V and –0.1 V, respectively, (temperature 700 °C, $p(O_2)$ 0.1 bar)

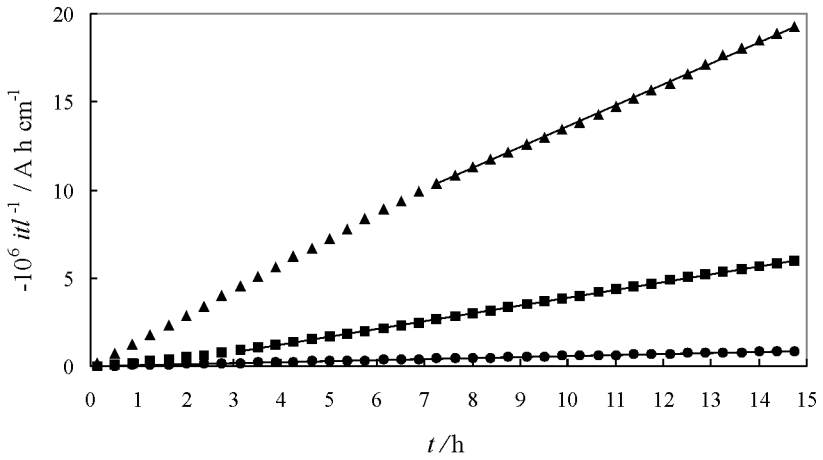

Fig. 10. Dependences of the itl^{-1} product on the time of polarization for the Au quasi-point electrode placed at the YSZ electrolyte. Triangles, squares and circles correspond to the polarization electrode potentials: –0.3 V, –0.2 V and –0.1 V, respectively, (temperature 700 °C, $p(O_2)$ 0.1 bar)

The dependences of the currents drawn from the electrode under the polarization of –0.1, –0.2 and –0.3 V on time for YSZ and GDC electrolytes are shown in Figs. 8 and 9, respectively. The current values were normalized vs. the TPB lengths, determined according to the procedure described earlier in this paper. Two distinct features of these dependences can be seen: the currents need a relatively long time to be stabilized when the electrode is polarized (i). It is especially clearly seen for the intermediate value of the polarization (–0.2 V); the currents, normalized vs. the TPB length, for the GDC electrolyte are distinctly higher than these for the YSZ electrolyte (ii).

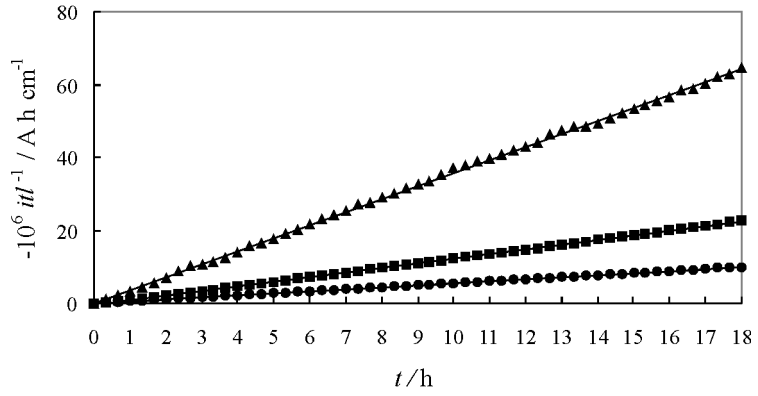

Fig. 11. Dependences of the itl^{-1} product on the time of polarization for Au quasi-point electrode placed at the GDC electrolyte. Triangles, squares and circles correspond to the polarization electrode potentials: –0.3 V, –0.2 V and –0.1 V, respectively, (temperature 700 °C, $p(O_2)$ 0.1 bar)

Because of the phenomenon described in entry (i), we made an attempt to estimate the asymptotic values of the currents $(il^{-1})_\infty$ i.e., their values after infinitely long time of polarization. From our previous numerous data obtained for the YSZ electrolyte [22], we have found that the character of the current–time dependence in this case could be fitted (after passing over some initial points) with the hyperbolic equation

$$il^{-1} = (il^{-1})_\infty \pm \frac{\text{const}}{t} \tag{7}$$

Hence, the most convenient way to estimate the $(il^{-1})_\infty$ values is to calculate the slopes of the linear regressions (itl^{-1}) vs. t fitted to the experimental points. These dependences, for the data presented in Figs. 8 and 9, are shown in Figs. 10 and 11, respectively. The linear character of the dependences shown in Figs. 10 and 11 confirms that the assumed Eq. (7) can be used to describe the behaviour of the electrode performance under polarization.

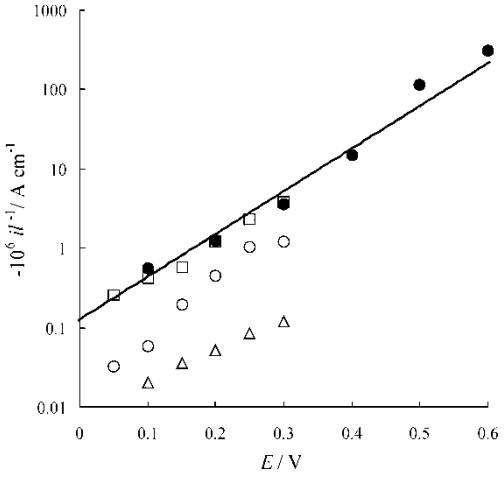

Fig. 12. The Tafel plots of $(il^{-1})_\infty$ vs. E for the GDC (full circles, $p(O_2) = 0.1$ bar) and YSZ electrolytes (empty squares, circles and triangles correspond to $p(O_2)$ equal to 1.0, 0.1 and 0.01 bar, respectively, temperature 700 °C)

The Tafel plots of $\log(il^{-1})_\infty$ vs. E for the YSZ and GDC electrolytes are presented in Fig. 12. In this figure, we additionally present the data for the YSZ electrolyte obtained under the partial pressures of O_2 equal to 0.01 and 1.0 bar. The calculated values of the apparent exchange currents normalized vs. the TPB length and Tafel slopes are given in Table 2. As can be seen, at the partial pressure of oxygen equal to 0.1 bar, the apparent exchange current for GDC is distinctly higher than that for YSZ. This favours use of GDC over YSZ in IT SOFC. The calculated Tafel slopes are similar for all the considered cases, pointing to much the same mechanism of the oxygen reduction for both the electrolytes investigated [23]. Under this assumption, the average value of αn could be calculated for all the data presented in Table 2. It is equal to $\alpha n = 1.05 \pm 0.21$, indicating that α is approximately equal to 0.5.

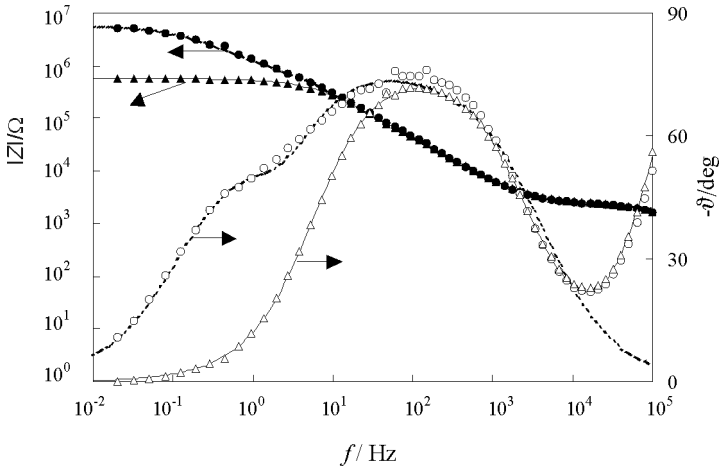

Fig. 13. Bode plots for the Au quasi-point electrode placed at the YSZ electrolyte (●, ○ unpolarized electrode, ▲, △ electrode polarized at –0.3 V; temperature 700 °C, $p(O_2)$ 0.1 bar)

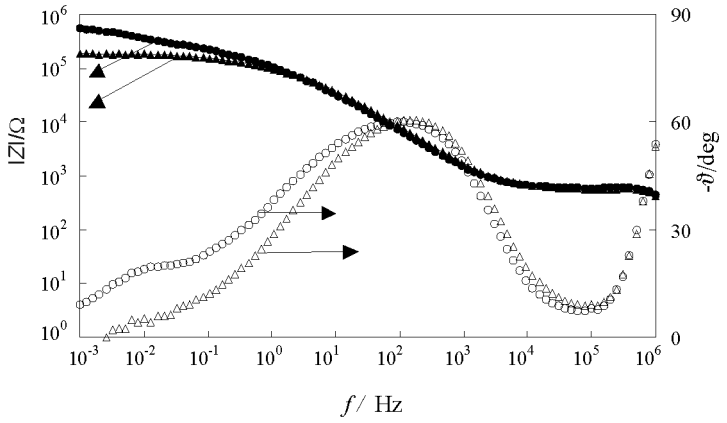

Fig. 14. Bode plots for the Au quasi-point electrode placed at the GDC electrolyte (●, ○ unpolarized electrode, ▲, △ electrode polarized at –0.3 V; temperature 700 °C, $p(O_2)$ 0.1 bar)

A similar character of the impedance Bode plots for the unpolarized and polarized electrodes at YSZ and GDC (disappearance of the additional branch at the phase dependence for the polarized electrodes) also confirms this similarity (Figs. 13 and 14). The complex impedance plots, normalized vs. the TPB length, are shown in Figs. 15 and 16 for the YSZ and GDC, respectively. The lower impedances observed for the GDC than YSZ can be correlated with the apparent exchange currents given in Table 2. The impedance data are now under detailed analysis which, together with the data obtained for an extended range of O_2 partial pressures and other electrode materials, will be presented in our further paper.

Table 2. Exchange currents and αn factors determined from The Tafel plots of the oxygen electrode reaction

Electrolyte	$p(O_2)$/bar	$-10^9\, i_0 l^{-1}$/A·cm^{-1}	αn
GDC	0.1	100.8	1.11
YSZ	0.01	6.7	0.84
YSZ	0.1	15.4	1.32
YSZ	1.0	137	0.92

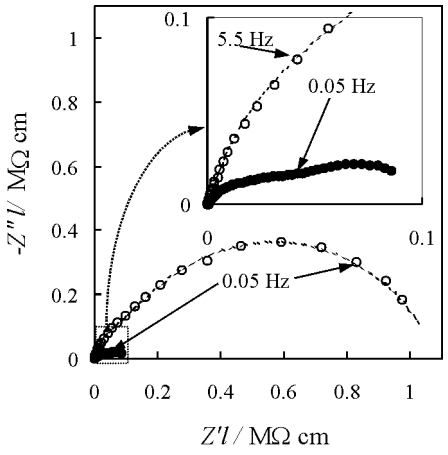

Fig. 15. Impedance complex plots of the unpolarized Au quasi-point electrode placed on the YSZ (○) and GDC (●) electrolyte (temperature 700 °C, polarization potential 0 V, $p(O_2)$ 0.1 bar)

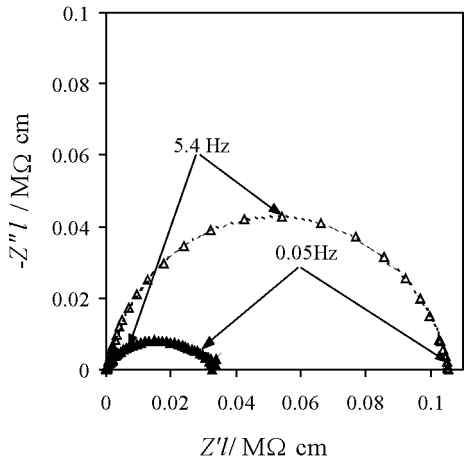

Fig. 16. Impedance complex plots of the polarized Au quasi-point electrode placed at the YSZ (△), and GDC (▲) electrolyte (temperature 700 °C, polarization potential –0.3V, $p(O_2)$ = 0.1 bar)

4. Conclusions

The paper presents the data obtained for the Au quasi-point electrodes in contact with two various electrolytes: yttria stabilized zirconia and gadolinia doped ceria. To

normalize the data obtained for the YSZ and GDC electrolytes, the procedures of determining the TPB length were discussed. Finally, the values of TPB lengths were estimated based on admittance measurements and specific conductivity of the electrolyte sample determined by EIS measurements. The CA dependences recorded for the durations lasting several hours showed that GDC is a better electrolyte for IT – SOFC than YSZ. Similar conclusions were drawn from the results obtained with EIS spectroscopy.

Acknowledgement

This work was financially supported by the AGH University of Science and Technology in Cracow under the contract No. 10.10.210.74.

References

[1] MINH N.Q., TAKAHASHI T., *Science and Technology of Ceramic Fuel Cells*, Elsevier, Amsterdam, 1995.
[2] GELLINGS P.J., BOUWMEESTER H.J.M., *The CRC Handbook of Solid State Ionics Electrochemistry*, CRC Press, Boca Raton, FL, 1997.
[3] TULLER H.L., Solid State Ionics, 131 (2000), 143.
[4] STEELE B.C.H., Solid State Ionics, 129 (2000), 95.
[5] MOGENSEN M., SAMMES N.M., TOMPSETT G.A., Solid State Ionics, 129 (2000), 63.
[6] JACOBSEN T., ZACHAU-CHRISTIANSEN B., JØRGENSEN M., Electrochim. Acta, 46 (2001), 1019.
[7] JACOBSEN T., BAY L., Electrochim. Acta, 47 (2002), 2177.
[8] BREITER M. W., LEEB K., FAFILEK G., J. Electroanal. Chem., 434 (1997), 129.
[9] PĘDZICH Z., HABERKO K., Ceramic Int., 20 (1994), 85.
[10] PAWŁOWSKI A., BUĆKO M. M., PĘDZICH Z., Mater. Res. Bull., 37 (2002), 425.
[11] DUDEK M., MOLENDA J., Mater. Sci.-Poland, 24 (2006), 45.
[12] STELLE B.C.H., *Oxygen Ion Conductors*, [in:] *High Conductivity Solid Ionic Conductors*, T. Takahasi (Ed.), World Scientific, Singapore, 1989, p. 402.
[13] KUDO T., OBAYASHI H., J. Electrochem. Soc., 122 (1975), 142.
[14] YAMAMOTO O., Electrochim. Acta, 45 (2000), 2423.
[15] KUDO T., OBAYASHI H., J. Electrochem. Soc., 123 (1976), 415.
[16] INABA H., TAGAWA H., Solid State, 83 (1996), 1.
[17] RIESS I., BRAUNSHTEIN D., TANNHAUSER D.S., J. Am. Ceram. Soc., 64 (1981), 479.
[18] BALAZS G. B., GLASS R.S., *Conductivity measurements of ceria based solid electrolytes using AC impedance*, [in:] *Ionic and Mixed Conducting Ceramics*, T.A. Ramanarayanan, W.L. Worrell, H.L. Tuller (Eds.), Proc. 2nd Intern Symp., The Electrochemical Society, 1994, p. 478.
[19] EGUCHI K., SETOGUCHI T., INOUE T., ARAI H., Solid State Ionics, 52 (1992), 165.
[20] TIANSHU Z., HUANG H., KILNER J., HING P., Solid State Ionics, 148 (2002), 567.
[21] NEWMANN J., Electrochem. Soc., 113 (1966), 501.
[22] TOMCZYK P., ŻUREK S., MOSIAŁEK M., in preparation.
[23] BARD A.J., FAULKNER L.F., *Electrochemical Methods Fundamental and Applications,* Wiley, New York, 1980.

Received 28 April 2007
Revised 16 February 2008